Front. Optoelectron. China 2009, 2(2): 233–238
DOI 10.1007/s12200-009-0042-8

RESEARCH ARTICLE

FBG sensing temperature characteristic and application in oil/gas down-hole measurement

Shaomin LI[1], Xiaoying LIU (✉)[1], You LI[2], Shenlong YANG[1], Chong LIU[1]

1 College of Optoelectronic Science and Engineering, Huazhong University of Science and Technology, Wuhan 430074, China
2 School of Foreign Languages, Wuhan University of Technology, Wuhan 430079, China

Abstract Fiber Bragg gratings (FBGs) have been used to sense numerous parameters such as strain, temperature, and pressure. Cost-effective multipoint measurements have been achieved by connecting FBGs in parallel, serial, and other topologies as well as by using spatial, wavelength, and time-domain multiplexing techniques. This paper presents a method of measuring temperature of the oil/gas down-hole. Detailed contents include the basic theory and characteristics of fiber gratings, analysis of the sensing mechanism of fiber-optic gratings, and the cross-sensitivity effect between temperature and strain; the method of making the light-source of the fiber-optic gratings and the technology of measuring wavelength shift, building an experimental system of the temperature measurement, and dealing with the experimental data. The paper makes a comparison of several kinds of FBG sensing systems used in oil/gas down-hole to measure temperature and the analysis of the experimental results of building the temperature measurement experimental system. It demonstrates that the fiber-optic grating sensing method is the best choice in all methods of measuring temperature in oil/gas down-hole, which has a brilliant applied prospect.

Keywords fiber-optic gratings, oil/gas down-hole, cross-sensitivity effect, sensor, temperature measurement

1 Introduction

An in-fiber Bragg grating is constructed by varying the refractive index of the core lengthwise along the fiber [1]. Light of the specified wavelength traveling along the fiber is reflected from the grating back in the direction from which it came from. Wavelengths that are not selected passes through with little or no attenuation. The reflection or transmission peak wavelength of photonic band gap (PBG) is related to the modulation cycle of the fiber's refractive index. The change of outside temperature or strain will affect the modulation cycle and the refractive index in the core of the fiber. Thus, it will have an effect on the change of the reflection or transmission wavelength of the fiber Bragg grating (FBG) and that is the basic working principle of FBG [2].

Compared with common machinery and electronic sensors, the FBG sensors have many eminent characteristics like anti-electromagnetic interference (anti-EMI), good electrical insulation, corrosion resistant, small volume, low transmission loss, great capacity, wide range of measurement, etc. The oil industry is faced with high-loss, strong-corrosion inflammable, and explosive condition; as a result, the sensors used in this area have a higher demand. Such kinds of electrical sensors used in monitoring oil and gas cans, wells, and pipes have unsafe factors. Since FBG sensors is in essence secure, they have generated much interest for usage as sensors to measure strain, temperature, and other physical parameters in bad environment. For this reason, the FBG sensors are very suitable to be used in oil industry [3].

In this paper, the authors present a method in measuring temperature of the oil/gas down-hole and solve the problem of the cross-sensitivity effect between temperature and strain.

2 Theory and principle of FBG sensors

2.1 Sensing mechanism of FBG

The FBG is formed by changing the refractive index of the fiber core area so as to produce a low periodic disturbance. For the disturbance, it only can influence a small section of the spectrum (the typical spectral width is about 0.05–0.3 nm), while the other transmission light can hardly be

Received November 20, 2008; accepted December 29, 2008

E-mail: liuxy@mail.hust.edu.cn

influenced. Therefore, the incident wave will be reflected back in corresponding frequency when the broadband light is transmitting in FBG. The center wavelength reflected back is as follows:

$$\lambda_B = 2n_{eff}\Lambda, \tag{1}$$

where n_{eff} represents the effective refractive index of FBG fiber core, and Λ is the pitch cycle of FBG.

By means of total differential, Eq. (1) can be expressed as

$$\Delta\lambda_B = 2\Delta n_{eff}\Lambda + 2\Delta\Lambda n_{eff},$$
$$\frac{\Delta\lambda_B}{\lambda_B} = \frac{\Delta\Lambda}{\Lambda} + \frac{\Delta n_{eff}}{n_{eff}}. \tag{2}$$

Under common conditions, as shown in Fig. 1, the FBG sensor is in a state in which the axial stress field σ, uniform temperature field T, and isotropic fluid static pressure field P are simultaneously functioning on it.

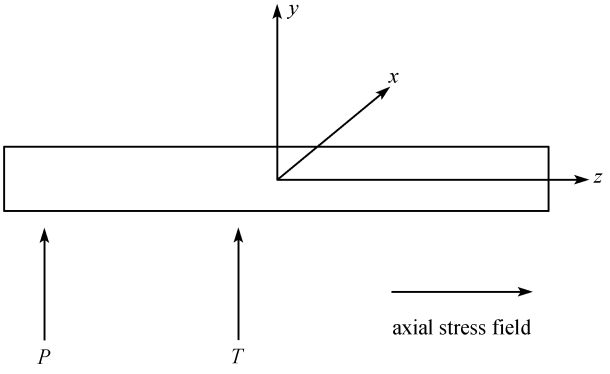

Fig. 1 Sensing schematic diagram of FBG in free conditions

As mentioned in Eq. (2),

$$\frac{\Delta\Lambda}{\Lambda} = \xi_Z + \alpha\Delta T = \left[\frac{\sigma_Z}{E} - \frac{(1-2v)P}{E}\right] + \alpha\Delta T, \tag{3}$$

$$\frac{\Delta n_{eff}}{n_{eff}} = \frac{1}{n_{eff}}\left[\left(\frac{\partial n_{eff}}{\partial\xi}\right)\Delta\xi + \left(\frac{\partial n_{eff}}{\partial T}\right)\Delta T + \left(\frac{\partial^2 n_{eff}}{\partial\xi\partial T}\right)\Delta\xi\Delta T\right], \tag{4}$$

where the first term of right equal sign in Eq. (4) represents the relative refractive index variation caused by elasto-optic effect; the second term represents the relative refractive index variation caused by thermo-optical effect and then introduce the thermal-optic coefficient ξ $\left[\xi = \frac{1}{n_{eff}}\left(\frac{\partial n_{eff}}{\partial T}\right)\right]$; the third term is strain-temperature cross-sensitivity, which is always seen as high-order term and can be neglected.

Substituting Eqs. (3) and (4) into Eq. (2), according to the acknowledgement of elastic mechanics, we can get

$$\frac{\Delta\lambda_B}{\lambda_B} = \frac{n_{eff}^2}{2}\left\{\frac{P_{11}}{E}[v\sigma_Z + (1-2v)P] + \frac{P_{12}}{E}[(v-1)\sigma_Z + 2(1-2v)P]\right\} + \xi\Delta T + \left[\alpha\Delta T + \frac{\sigma_Z}{E} - \frac{(1-2v)P}{E}\right], \tag{5}$$

where σ_Z is the axial strain; P_{11} and P_{12} are the photoelasticity coefficients of the optical fiber materials; E and v represent the elasticity modulus and the Poisson ratio of the optical fiber materials, respectively; α and ξ respectively represents the thermal expansion coefficient and thermo-optic coefficient of the optical fiber materials; ΔT is the variance of temperature; and P is the hydrostatic pressure.

1) Considering only the action of temperature of $\Delta T \neq 0$, $P = 0$, $\sigma_Z = 0$, Eq. (5) can be transformed as follows:

$$\frac{\Delta\lambda_B|_T}{\lambda_B} = (\xi + \alpha)\Delta T.$$

The corresponding sensitivity of temperature sensor is

$$K_T = \frac{\Delta\lambda_B|_T}{\Delta T} = (\xi + \alpha)\lambda_B.$$

2) Considering only the action of axial stress σ_Z, Eq. (5) can be transformed as

$$\frac{\Delta\lambda_B|_{\sigma_Z}}{\lambda_B} = \left[\frac{n_{eff}^2}{2}(P_{11}v + P_{12}v - P_{12}) + 1\right]\frac{\sigma_Z}{E}.$$

The corresponding strain sensitivity coefficient is

$$K_{\sigma_Z} = \frac{\Delta\lambda_B|_{\sigma_Z}}{\sigma_Z} = \left[\frac{n_{eff}^2}{2}(P_{11}v + P_{12}v - P_{12}) + 1\right]\frac{\lambda_B}{E}.$$

3) Considering only the action of hydrostatic pressure P, Eq. (5) can be simplified as

$$\frac{\Delta\lambda_B|_P}{\lambda_B} = \frac{(1-2v)P}{E}\left[n_{eff}^2\left(\frac{P_{11}}{2} + P_{12}\right) - 1\right].$$

The corresponding sensitivity coefficient of hydrostatic pressure is

$$K_P = \frac{\Delta\lambda_B|_P}{P} = \frac{(1-2v)\lambda_B}{E}\left[n_{eff}^2\left(\frac{P_{11}}{2} + P_{12}\right) - 1\right].$$

Eq. (5) can be expressed as follows in terms of sensitivity coefficient:

$$\Delta\lambda_B = K_T\Delta T + K_{\sigma_Z}\sigma_Z + K_P P.$$

2.2 Analysis on strain and temperature cross-sensitivity problem of FBG sensors

From the analysis above, the center wavelength of FBG is extremely sensitive to strain and temperature. While measuring one parameter, the other parameter will certainly be affected. Therefore, solutions to the strain

and temperature cross-sensitive problem of FBG and simultaneous measurement technology on strain and temperature are keys to the further development of FBG sensors [4].

To solve the strain and temperature cross-sensitive problem of FBG strain sensors, a method based on a reference FBG was presented. When the reference FBG is in series with an FBG strain sensor, the structure strain can be acquired by the relative wavelength shift of these two FBG sensors. Solutions were mostly based on three thoughts: double-wavelength matrix algorithm [5], dual-parameter matrix algorithm [6], and strain or temperature compensation method [7].

Based on the analysis above, at present, the existing FBG temperature (strain) measurement unit is made of two gratings. Not only does this unit have a high cost, but its measurement accuracy is limited, and it is also difficult to measure temperature and strain at the same time. During the distributed measurement of the temperature (strain) in actual oil/gas down-hole, we used a real-time measurement of temperature (strain) at equidistant measuring points in a section of vertical distance. In this paper, a new measurement method was suggested. When measuring the temperature of the distribution points, we have the single FBG sensor packaged so as not to make it sensitive to the strain. Then, the packaged FBG sensors were connected in series one by one, so as to realize the distributed temperature measurement. The principle of measuring strain is the same.

3 Light source and signal demodulation

3.1 LED light source

In the whole system of the experiment, we used a light-emitting diode (LED) light source of the wide spectrum. The excitation methods of the LED laser mostly used electric injection, and the increase of the current is approximately expressed linearly with the output power [8]. Different from the semiconductor laser, the LED does not have threshold current, but when the working current reaches a certain value, the curve of output power current has a distortion.

Figure 2 shows the *P-I* curve of the LED.

The coefficient of constant current S_1 is

$$S_1 = \frac{\Delta I_L}{I_L} \Big/ \frac{\Delta U_1}{U_1}, \tag{6}$$

where I_L is the current flowing through the laser. According to Eq. (6), it can be inferred that the smaller S_1 is, the less the influence of I caused by the change in U_1, and the better the performance of the current stabilization.

Figure 3 shows the driving circuit of the light source for LED.

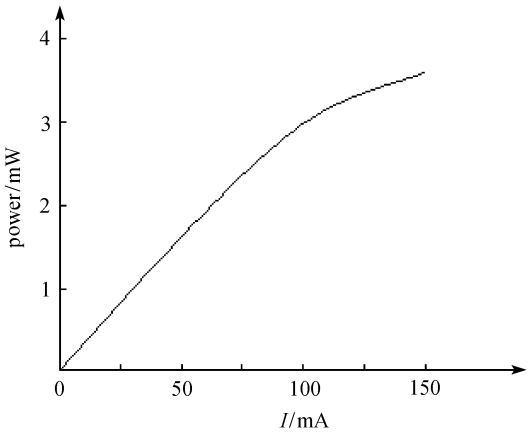

Fig. 2 *P-I* curve of LED

3.2 Demodulation technique of FBG sensors

The key technology of FBG sensor is undoubtedly the detection of the wavelength shift. Until now, there are many kinds of detection methods, including spectrometer detection method, match grating method, tunable Fabry-Perot (F-P) method, non-equilibrium Mach-Zehnder interferometer tracing method, tunable laser method, etc. [9].

The sensing system constructed by FBG should have a sophisticated wavelength or the change in the wavelength detection device in which the sensing volume takes the microdisplacement of the wavelength as a vector.

We suggested a tunable F-P cavity filter to detect the wavelength shift. The characteristics of the tunable F-P cavity filter free spectral range (FSR) is larger than the working spectrum of FBG which can guarantee that the reflected signal of FBG to be always detected by the F-P cavity. The F-P cavity can be used as a narrowband filter. In a certain wavelength extent, only when a parallel light incident beam in F-P cavity and in some special wavelength satisfies coherent conditions, interference will happen, and the coherent maximum is generated. By using the characteristics of the F-P cavity, we can detect the reflected wavelength of the FBG sensor. Its working principle is shown in Fig. 4.

The light given off by the broadband source passes through the optical circulator and is transmitted to the FBG sensor. And then, the light reflected by FBG sensor is introduced to the F-P cavity. Its structure diagram is shown in Fig. 5. First, the lens L1 changes the incident light from the fiber into parallel light incidence to the F-P cavity. Then, the emergent light passing by the lens L2 transmits together to the sensor. One of two high reflectors forming the F-P cavity is fixed, the other can move, and its back side is pasted by a piezoelectric ceramics (PZT). Put a scanning voltage to the PZT, and it will stretch so that the cavity length of the F-P cavity will change. If the transmission peak wavelength of the F-P cavity coincides

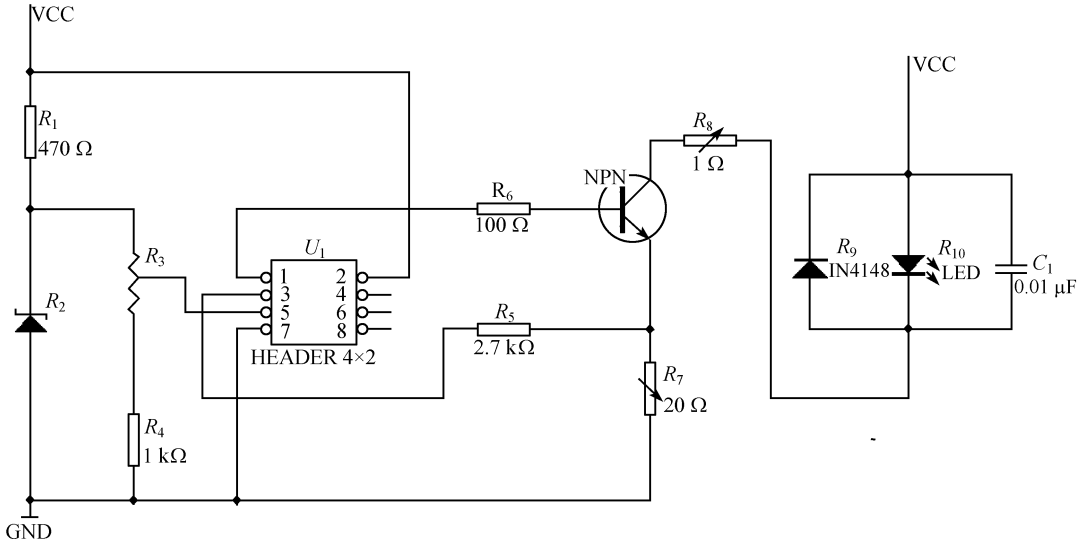

Fig. 3 Driving circuit of light source for LED

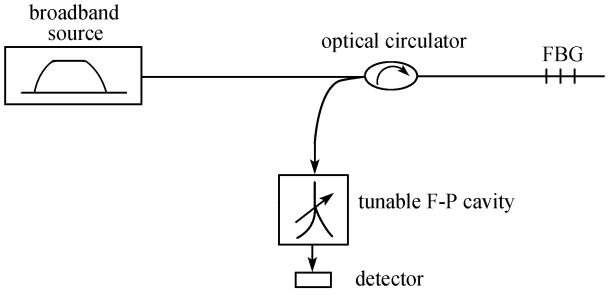

Fig. 4 Principle chart of tunable F-P cavity measuring reflected wavelength of FBG

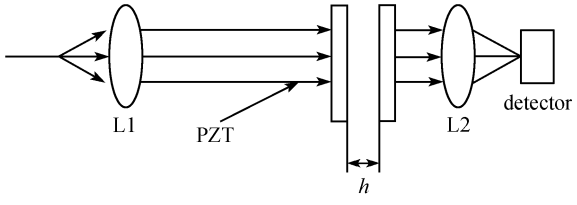

Fig. 5 Schematic diagram of tunable F-P cavity

with the reflected wavelength of FBG, the detector can sense the maximum light intensity. In this case, the voltage V which was put on PZT represents the reflection wavelength of FBG.

When detecting wavelength by F-P cavity, we have to make reasonable design of the constant such as F-P cavity's facet reflectivity, distance between two microscopes, etc., which is according to the range of measurable optical wavelengths, resolving power, etc. [10].

4 Experimental system

Figure 6 shows the schematic diagram of the experimental system. The working process is described as the broadband light given off by the light source passes through optical circulator and is transmitted by the fiber. Then, it reaches the FBG sensors one by one. The narrow spectrum that satisfies the Bragg condition will be reflected back, and the center wavelength of which (Bragg wavelength) has already occurred an offset relative to its initial wavelength (the center wavelength not influenced by measured data of temperature and axial strain). Actually, the measured parameters that are carried again passes through the optical circulator and the single mode fiber. Then, it arrived at the FBG wavelength shift detection system to continue detecting wavelength shift. Figure 7 shows the reflectance spectrogram of three FBG sensors. The instrument of detecting the wavelength shift is the MS9710C spectrometer produced by Anritsu.

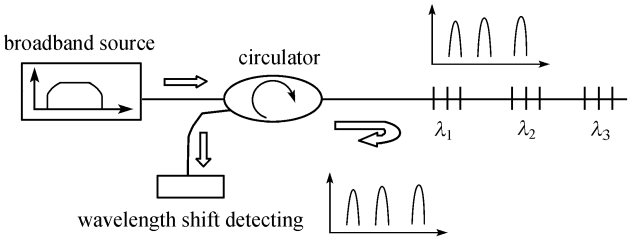

Fig. 6 Fundamental principle block diagram of FBG sensor

In the actual experiment, we used the experimental system shown in Fig. 8.

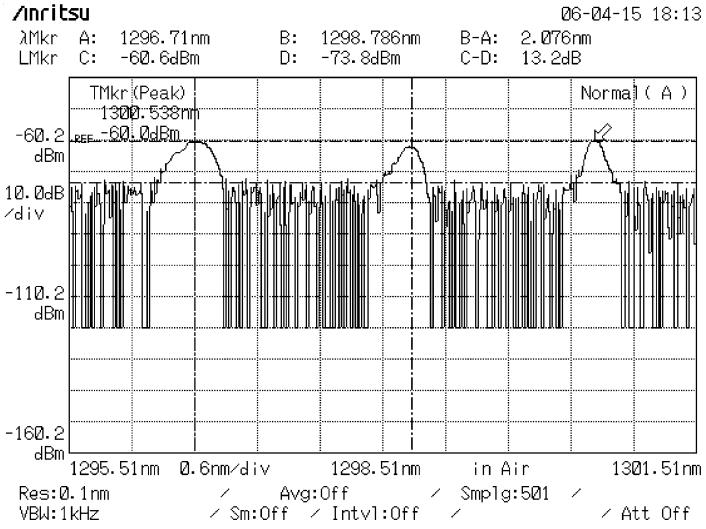

Fig. 7 Reflectance spectrogram of three FBG sensors

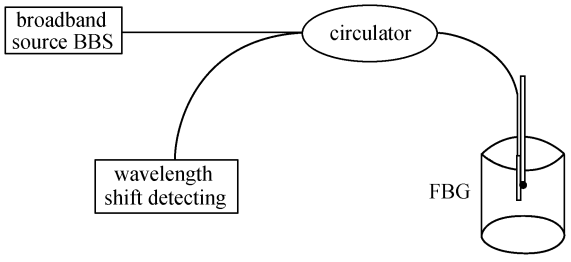

Fig. 8 Fundamental principle block diagram of FBG sensor

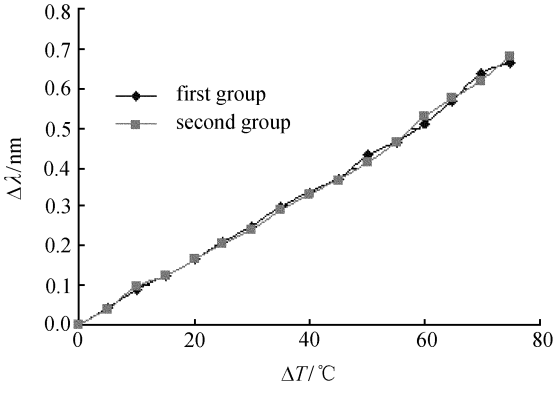

Fig. 9 Curves of wavelength shift and temperature variation

5 Experimental data processing

In order to get the FBG sensor's temperature characteristic, we build the experimental system according to Fig. 8. The FBG sensor's center wavelength is 1302 nm. The instrument of detecting the wavelength shift is the MS9710C spectrometer produced by Anritsu. The center wavelength of the broadband light source is 1300.0 nm, while the bandwidth is 50 nm. Figure 9 shows the curve between the relative shift of the reflected center wavelength $\Delta\lambda$ and the temperature variation ΔT from the experiment.

We measured a change of temperature with each 5°C variation in the range 20°C to 95°C and made two measurements. The fitting linear equation is given by means of linear fitting for the curve:

$$\Delta\lambda_B = 0.0089\Delta T - 0.012. \quad (7)$$

From Eq. (7), we can know the sensitivities of temperature sensor K_T is 0.0089 nm/°C, and the FBG sensor's sensitivities of temperature sensor K_T is 10.3 pm/°C. The order of magnitude of the two coefficients is the same, while the concrete coefficient value is not. This is because the elasto-optical coefficient, thermal expansion coefficient, and the material parameters of Young's modulus are different from each other. However, the order of magnitude of the two coefficients is the same, which shows that it is a correct method.

Draw the curve according to Eq. (7), compare it with original curve, and show them in Fig. 10.

We can see that the fitted linear curve is comparatively comfortable to the testing results. Also, the experimental results are basically identical to the theoretical analysis, which presents preliminary proof of the correctness of FBG temperature sensing models. However, there is error in fitting formula. The causes of errors are many, such as the reading of center wavelength that is always changing when measuring center wavelength, and the recording data that is just the mean of several jump numbers. Because the

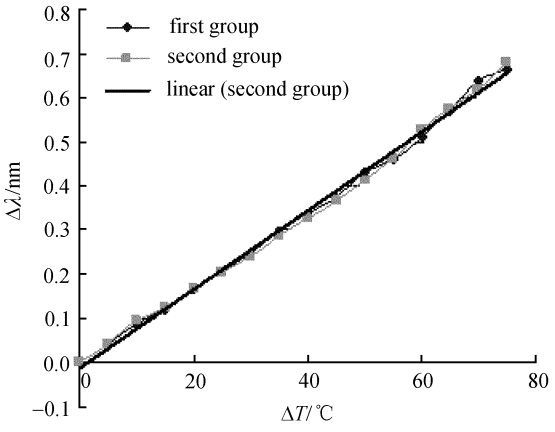

Fig. 10 Comparison with fitting linear curve and experimental curve

reading of center wavelength is slower than the changing of center wavelength, thus, it brings error to the measurement.

A linear relationship holds in the data curve of the FBG sensor excluded from the condition of stress influence. When it is applied, in order to measure the distributed temperature change down-hole, we made the packaged FBG sensors connected in series so as to measure the wavelength shift of different points.

6 Conclusion

This paper presents the sensing mechanism of fiber-optic gratings and analysis of the cross-sensitivity effect between temperature and strain. The LED light source of the wide spectrum was designed. We experimentally demonstrated a temperature sensor system and research on its temperature characteristic. The curve of wavelength shift and temperature variation from the FBG sensor is given. We described its application in oil/gas down-hole measurement by connecting the packaged FBG sensors in series. By using the wide spectrum LED light source and tunable F-P cavity filter, we can detect the wavelength shift. In the meantime, the distributed temperature measurement is realized. Besides, the analysis on the curve of wavelength shift and temperature variation proves validity of the measurement method.

References

1. Bi W B. Strain sensor using optical fiber unsymmetrical F-P cavity and the characteristic analysis. Chinese Journal of Lasers, 2000, 9 (2): 140–147 (in Chinese)
2. Kersey A D, Davis M A, Patrick H J, LeBlanc M, Koo K P, Askins C G, Putnam M A, Friebele E J. Fiber grating sensors. Journal of Lightwave Technology, 1997, 15(8): 1442–1462
3. Zhang X D. Fiber optic grating sensing technology and its application on the measurement of oil/gas down-hole. Dissertation for the Doctoral Degree. Xi'an: Graduate School of Chinese Academy of Sciences (Xi'an Institute of Optics and Precision Mechanics of Chinese Academy of Sciences), 2004, 3–6 (in Chinese)
4. Bhatia V, Campbell D, Claus R O, Vengsarkar A M. Simultaneous strain and temperature measurement with long-period gratings. Optics Letters, 1997, 22(9): 648–650
5. Zhang Z J, Wang C M. Investigation of the transfer matrix of the fiber gratings. Acta Photonica Sinica, 2007, 36(6): 1073–1077 (in Chinese)
6. Tan H, Devol T A. Development of a flow-cell alpha detector utilizing microencapsulated CsI:Tl granules and silicon PIN-photodiodes. IEEE Transactions on Nuclear Science, 2002, 49(3): 1243–1248
7. James S W, Dockney M L, Tatam R P. Simultaneous independent temperature and strain measurement using in-fiber Bragg grating sensors. Electronics Letters, 1996, 32(12): 1133–1134
8. Chen H X, Ni E D, Liu L. Information transfer and drive of a LED automobile light source. Journal of Wuhan University of Technology (Information and Management Engineering), 2005, 27(1): 143–146 (in Chinese)
9. Huang C, Jing W C, Liu K, Zhang Y M, Peng G D. Demodulation of fiber Bragg grating sensor using cross-correlation algorithm. IEEE Photonics Technology Letters, 2007, 19(9): 707–709
10. Pu H T, Jiang W C, Li X W, Chen J P, Qin L P. Studies on tunable F-P cavity based on doped unsaturated polyester. Journal of Functional Materials, 2005, 36(1): 118–120 (in Chinese)